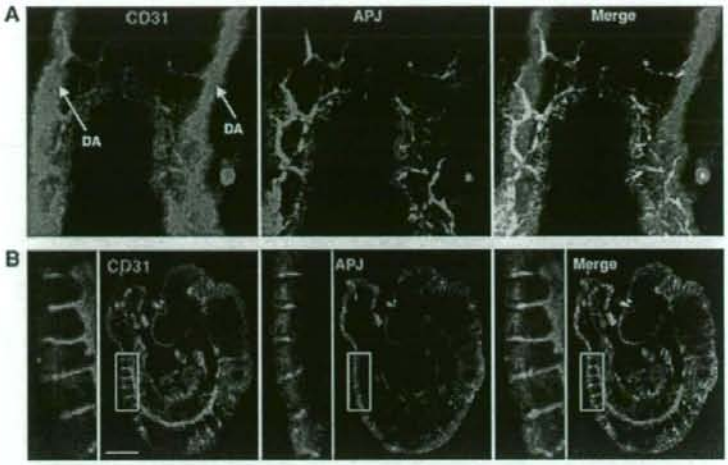

Figure 6 Expression of APJ in embryo. (**A**) Whole-mount staining of E8.5 mouse embryo with anti-CD31 (red) and anti-APJ (green) antibodies. (**B**) Staining of E9.5 mouse embryo section with anti-CD31 (red) and anti-APJ (green) Abs. The left panel shows high-power view of the area indicated by the box. Note that the DA stained by anti-CD31 Ab did not express APJ and APJ expressed on ECs sprouting from DA. Scale bar indicates 500 μm.

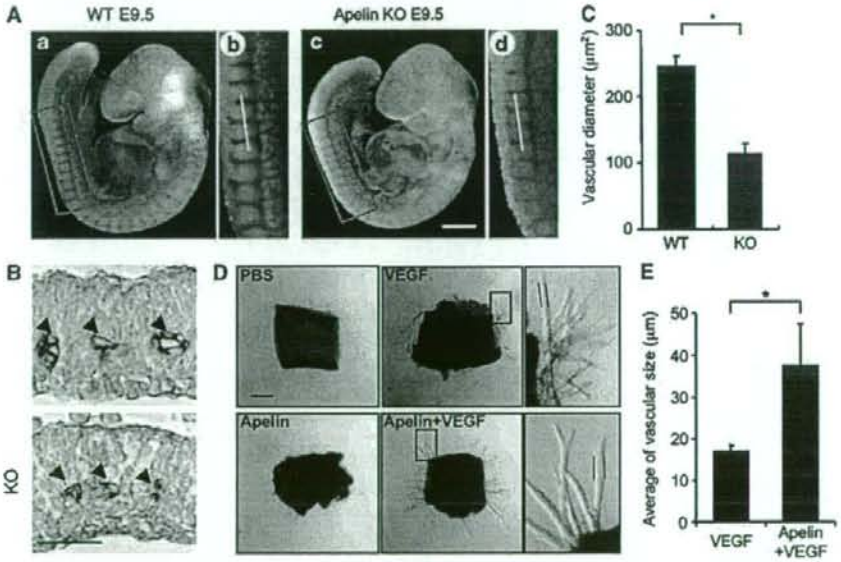

Figure 7 Defect of the enlargement in blood vessel caliber in apelin-deficient mice. (**A**) Whole-mount immunohistostaining of WT (a, b) and apelin-deficient (c, d) embryos at E9.5 with anti-CD31 Ab. (b) and (d) are higher magnifications of the areas indicated by the box in (a) and (c), respectively. Scale bar indicates 300 μm. (**B**) Sections containing ISVs (arrowheads) from WT and apelin-deficient (KO) embryos at E9.5 were stained with anti-CD31 antibody. The level of the sectioning position is indicated by a white bar in (b) and (d). Scale bar indicates 30 μm. (**C**) Quantitative evaluation of the vascular diameter of intersomitic blood vessels from apelin-deficient (KO) versus WT mice. $^*P<0.001$ (30 vessels from 5 embryos were examined). Details of the measurement of vascular diameter are shown in Supplementary Figure 7. (**D**) Representative pictures of microvessels sprouted from aortic ring using apelin-deficient mice. Aortic ring was cultured in the presence or absence of VEGF (10 ng/ml) or apelin (100 ng/ml). PBS was used as a negative control. Pictures in the right panel show a high-power view of the area indicated by the box, respectively. Scale bar indicates 300 μm. (**E**) Quantitative evaluation of the vascular size of sprouted microvessels from the aortic ring cultured as described in (D). Vascular size was measured as the length between two parallel lines as indicated in (D). $^*P<0.003$ ($n=30$).

absence of blood flow. It is known that blood flux regulates vessel size (Koller and Huang, 1999). Therefore, it is possible that shear stress may induce apelin expression in ECs. However, the results were contrary to our expectation. *In vitro* shear stress on HUVECs attenuated apelin mRNA expression in HUVECs (Supplementary Figure 13).

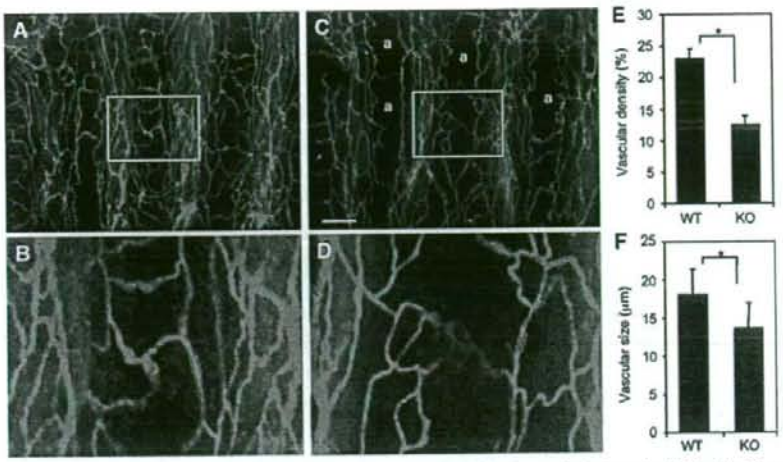

Figure 8 Lectin staining of tracheal blood vessels. (A–D) Comparison of tracheal blood vessels in 8-week-old WT (**A**, **B**) and apelin-deficient (**C**, **D**) mice stained by intravenous injection of fluorescein-labelled lectin. a in (C) means avascular area. (B) and (D) show a high-power view of the area indicated by the box in (A) and (C), respectively. Scale bar in (C) indicates 200 μm (A, C) and 60 μm (B, D). (**E**) Quantitative evaluation of vascular density from apelin-deficient (KO) versus WT mice. $^*P<0.001$. Vascular density from 10 random fields was counted. (**F**) Quantitative evaluation of vascular size of blood vessels in the trachea from apelin-deficient (KO) versus WT mice. Vascular size was measured as the length between two parallel red lines as indicated in (B) and (D). $^*P<0.001$ (100 vessels from 3 mice were examined).

Role of apelin in Ang1-induced enlargement of capillary size

We isolated apelin from ECs under the activation of Tie2 by Angl. Next, using apelin-deficient mice, we observed whether Angl-induced enlargement of blood vessels is suppressed in the absence of apelin. In this experiment, we mated apelin-deficient mice with Angl Tg mice and observed the caliber size of the capillaries in the dermis (Figure 9).

In apelin-deficient mice, the caliber size of the capillary in the dermis was narrower compared with that in WT mice (Figure 9A and B and Supplementary Figure 11). We confirmed that CD31-positive cells are from blood vessels but not from lymphatic vessels, by double staining with LYVE1, a specific marker for lymphatic ECs (Supplementary Figure 11). As previously reported (Suri *et al*, 1998), Angl Tg mice showed enlarged capillary formation in the dermis, but this effect of Angl was abolished by the lack of apelin (Figure 9A and B). However, apelin deficiency did not completely suppress Angl-induced enlargement of blood vessels, suggesting that other molecules upregulated by Tie2 activation might be involved in the caliber size determination of capillaries *in vivo*. On the other hand, the generation of extremely enlarged blood vessels, with a caliber size of more than $10^4\,\mu m^2$, observed in Angl Tg mice, was completely suppressed in the absence of apelin (Figure 9A and C). Therefore, we concluded that one of the molecules affected by Angl for enlargement of the capillary was apelin in ECs.

Apelin induces an enlarged endothelial sheet in P-Sp culture system

In vivo analysis suggested that apelin regulates the caliber change of blood vessels. Next, we observed blood vessel formation by using *in vitro* (P-Sp) organ culture system, which has previously been shown to mimic *in vivo* vasculogenesis and angiogenesis (Takakura *et al*, 1998, 2000). P-Sp explants from mice at E9.5 contain early developed DA. In the P-Sp culture system, ECs show two different morphologies. One is a sheet-like structure (vascular bed) that develops in the early stages of the culture. The other is a network-like structure, constructed from the ECs sprouting from the vascular bed. Previously, we identified that the sheet-like formation mimics vasculogenesis and the network formation mimics angiogenesis, which is a process of capillary sprouting from pre-existing vessels (Takakura *et al*, 2000). Therefore, as apelin-mutant embryos showed narrow ISVs, which were sprouted from the DA, this suggests that the P-Sp culture system can reproduce the *in vivo* effects of apelin.

In the P-Sp culture system, OP9 stromal cells were used as feeder cells for P-Sp explants. We induced apelin expression on OP9 cells (Figure 3B) and observed the effect. Compared to the control culture (Figure 10Aab), network-forming ECs became thick and the vascular density of the network area was high (Figure 10Acd), although the amount of branching was the same. By contrast, the suppression of apelin/APJ function, by blocking antibody against apelin, induced thin network formation by ECs (Figure 10Aef). When the network-forming area of ECs was evaluated, it was higher in apelin-expressing OP9 cells (OP9/apelin) than in control OP9 cells (OP9/vector); this effect by apelin was completely blocked by anti-apelin mAb (Figure 10Ag).

In the P-Sp culture system, we found that APJ is expressed in the network-forming ECs sprouted from the vascular bed as observed in the ISVs, but not in the ECs forming the sheet (Figure 10B). *In vitro* analysis indicated that the apelin/APJ system might affect cell-to-cell aggregation or assembly, and therefore we stained network-forming ECs by anti-VE-cadherin antibody. As observed in Figure 10C, apelin enhanced the assembly of ECs. Interestingly, in the control P-Sp culture, the network-forming endothelial layer, composed of one or two ECs, migrated in a peripheral direction along with the ECs at the tip (Figure 10Cab). On the other hand, when apelin was overexpressed on OP9 cells, many aggregated

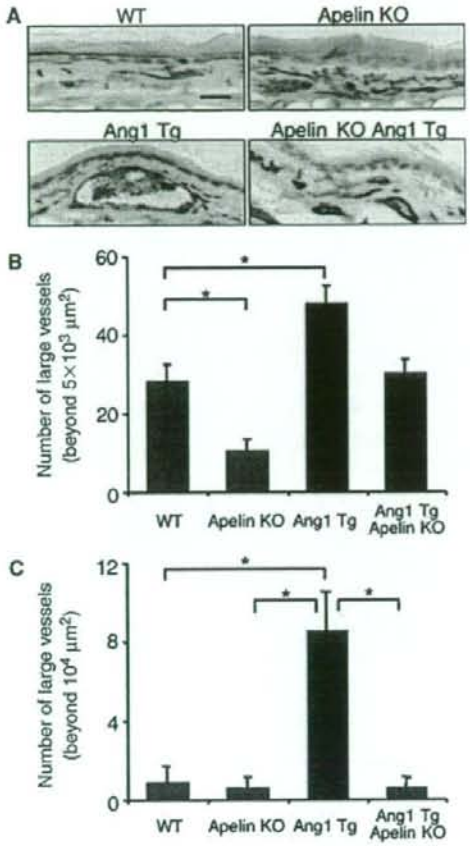

Figure 9 Apelin/APJ system is involved in Ang1-induced vascular enlargement. (**A**) Sections of ear skin stained with anti-CD31 mAb. Ear skin was prepared from 8-week-old WT, apelin-deficient (apelin KO), Ang1Tg mice, or apelin-deficient mice mated with Ang1Tg mice (apelin KO/Ang1 Tg). Scale bar indicates 30 μm. (**B**, **C**) Quantitative evaluation of the number of enlarged blood vessels composed of a luminal cavity of more than 5000 μm^2 (B) or more than 10^4 μm^2 (C) in the skin from mice as described in (A). Thirty random fields were observed from sections of three independent mice as described in (A). $^*P<0.01$.

ECs migrated along with the ECs at the tip (Figure 10Ccd), and this effect was completely suppressed by anti-apelin mAb (Figure 10Cef). These results indicated that apelin induces an enlarged endothelial sheet when angiogenesis is taking place.

Discussion

The knowledge of how vascular cells commit from their progenitor cells and generate a closed cardiovascular circulatory system has accumulated in recent years, mostly by the isolation and functional analysis of molecules associated with blood vessel formation. However, little is known regarding the molecular events that regulate EC morphogenesis, especially the caliber size determination of blood vessels. Data documented here, from both *in vitro* and *in vivo* analysis, showed that apelin regulates the enlargement of newly developed blood vessels during angiogenesis.

In angiogenesis, how blood vessels 'decide' their appropriate size is very important to the organization of the adjustment of tissue and organ demand for oxygen and nutrients. Our analysis clearly showed that APJ expression was induced by VEGF, which, in turn, is well known to be induced by tissue hypoxia (Liu *et al*, 1995). This indicates that, under tissue hypoxia, blood vessels have an opportunity to enlarge their size and the reduction of APJ expression finalizes the enlargement of blood vessel caliber under tissue normoxia. Indeed, in the retina, APJ was observed temporally in the radial vessels and the associated capillaries of retina from day 3 to day 12 after birth, but APJ expression on ECs was attenuated in the later stage (Saint-Geniez *et al*, 2002). As reported in the retina, we also found that APJ expression was observed in ECs sprouted from the DA and ECs on blood vessels in the neonatal dermis of mice (data not shown), but that it gradually disappeared with maturity. These expression patterns strongly suggested that APJ plays a spatio-temporal role in the maturation of blood vessels by transient expression on ECs of blood vessels where angiogenesis is taking place. Therefore, we concluded that one of the molecules associated with the regulation of blood vessel diameter was apelin in the ECs.

Based on our results presented here, it appears that VEGF, Ang1 and apelin regulate caliber size in a concerted fashion, as follows. Upon stimulation by VEGF, ECs sprouted from pre-existing vessels may express APJ. Subsequently, Ang1 stimulates these sprouted ECs to induce apelin expression. In the presence of both VEGF and apelin, the ECs start to proliferate, adhere and form contacts with each other through junctional proteins, and construct enlarged blood vessels. Apelin has been reported to induce angiogenesis in the Matrigel plug assay (Kasai *et al*, 2004) and also chemotaxis (Cox *et al*, 2006). In our experiments using the Matrigel plug assay, we found that apelin induced migration, rather than proliferation, of ECs (Supplementary Figure 14). Moreover, we confirmed that like VEGF, apelin modified the cytoskeleton structure (Supplementary Figure 15). Therefore, apelin may induce mobilization of ECs in the process of EC-to-EC assembly.

As we found, apelin deficiency suppressed the enlargement of ISVs during early embryogenesis. Furthermore, it has been reported elsewhere that Ang1 and VEGF are expressed in intersomitic or somitic tissues (Davis *et al*, 1996; Lawson *et al*, 2002) and that apelin is coexpressed with APJ-positive ECs in ISVs. Indeed both Tie2 and Ang1 mutant embryos showed impaired ISV formation (Dumont *et al*, 1994; Sato *et al*, 1995). Therefore, it appears that these three components may be involved in the regulation of caliber size change of the ISVs.

Transgenic overexpression of Ang1 in the keratinocyte induced enlarged blood vessels in the dermis (Suri *et al*, 1998) and administration of a potent Ang1 variant was also reported to induce enlargement of blood vessels (Cho *et al*, 2005; Thurston *et al*, 2005). Therefore, Ang1 expression may be a key determinant of caliber size during angiogenesis. Ang1 is usually produced from MCs in cells composing blood vessels (Davis *et al*, 1996), However, we previously reported that hematopoietic stem cells (HSCs) producing Ang1 migrate into avascular areas before the ECs start to migrate, and that this Ang1 from HSCs induces angiogenesis by promoting the chemotaxis of ECs (Takakura *et al*, 2000). Moreover, recently,

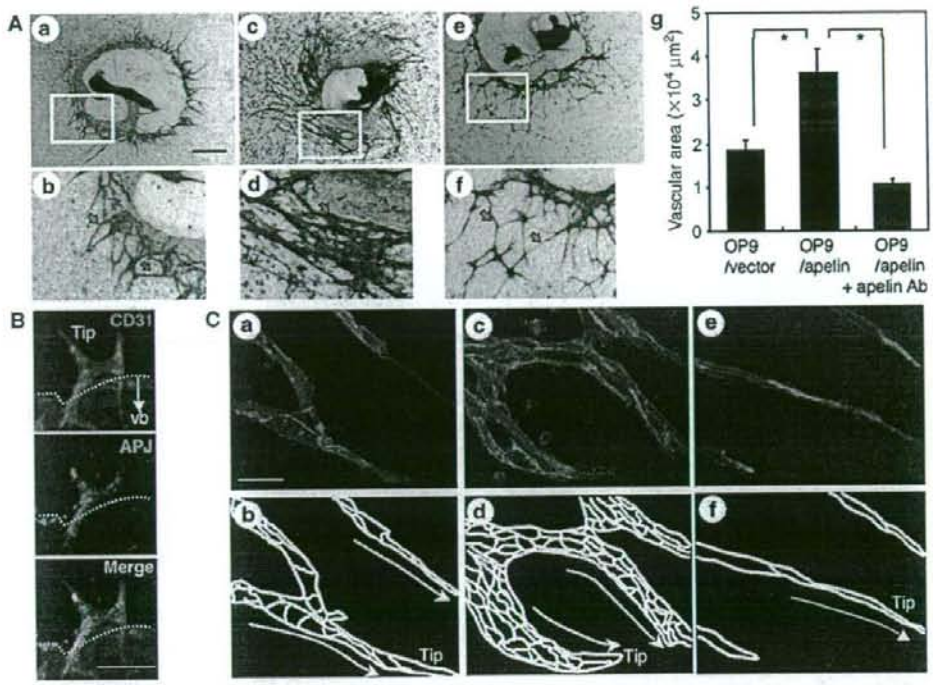

Figure 10 Effect of apelin on the P-Sp culture system. **(A)** Effect of apelin on the network-like structure of ECs in the P-Sp culture system. P-Sp explants from E9.5 mouse embryos were cultured for 7 days on OP9/vector (a, b) or OP9/apelin, in the presence of B220 control mAbs (c, d) or anti-apelin mAbs (e, f), and then stained with anti-CD31 mAb. (b), (d) and (f) are higher magnifications of areas indicated by the box in (a), (c) and (e), respectively. Arrows indicate network-forming ECs. Scale bar indicates 1 mm (a, c, e) or 200 μm (b, d, f). (g) Quantitative evaluation of the vascular network area cultured as above. Endothelial space per 500 μm length of network-forming ECs was measured in 10 random fields. $^{*}P<0.001$. **(B)** Expression of APJ in ECs of P-Sp culture. Cells on culture plates were stained with anti-CD31 (red) and anti-APJ (green) antibodies. Tip, tip EC. Dotted line indicates the border of the vascular bed (vb). Note APJ expressed on ECs forming a network-like structure. Scale bar indicates 100 μm. **(C)** Network-forming ECs derived from P-Sp explants cultured on OP9/vector (a, b), OP9/apelin in the presence of control B220 mAbs (c, d) or OP9/apelin in the presence of anti-apelin mAbs (e, f) for 7 days were stained with anti-VE-cadherin (red) mAbs. Scale bar indicates 20 μm. Because nuclear staining cannot distinguish the nuclei of ECs from those of OP9 cells, only VE-cadherin expression was revealed. Therefore, the EC-to-EC boundary expressed by VE-cadherin is presented (b, d, f). Tip, tip EC. Migration direction of tip EC is indicated by the arrow.

we found that HSCs induce enlargement of blood vessels observed in the fibrous cap surrounding tumors (Okamoto *et al*, 2005) and Angl from HSCs in embryos, as well as adults, induces structural stability of newly developed blood vessels as a physiological function during angiogenesis (Yamada and Takakura, 2006). Therefore, it is possible that Angl from the HSC population, which are frequently observed in ischemic regions, is the one source of Tie2 activation and results in the production of apelin from ECs.

It has been suggested that apelin mediates phosphorylation and activation of endothelial NO synthase in ECs, causing NO release from ECs (Tatemoto *et al*, 2001; Ishida *et al*, 2004). NO is well known to induce relaxation of MCs, resulting in dilation of blood vessels. Therefore, it is possible that apelin causes endothelium-dependent vasodilatation by triggering the release of NO from ECs. In our analysis, however, we observed that apelin induced enlarged cord formation of HUVECs on Matrigel, and enlarged spheroids of HUVECs in the liquid culture. These culture conditions do not contain MCs, which indicates that apelin can induce enlargement of blood vessels without affecting MCs.

Knockout studies of the apelin gene suggested that molecular cues other than apelin rescue the narrow caliber size of blood vessels by compensational upregulation, because in the early stage of embryogenesis the narrow caliber of ISVs, observed in apelin-mutant embryos, was rescued in the later stage (data not shown). As observed in apelin knockout mice, APJ mutant mice appeared healthy as adults (Ishida *et al*, 2004); however, the requisite role of the apelin/APJ system in blood vessel formation was reported in *Xenopus* (Cox *et al*, 2006; Inui *et al*, 2006). The reason of this discrepancy is not known, but functionally redundant ligand/receptor or signalling pathways may be present in mice.

Tube formation is a fundamental mechanism for organ and tissue generation in most major organs, such as lung and kidney, as well as the vasculature. The molecular mechanism involved in tube generation is not clearly understood. During angiogenesis, neovessels must be generated by both single cell hollowing and cord hollowing methods. Through the analysis of the precise functional relationship between the molecules described above including the apelin/APJ system, anatomically described diverse tube formation of the vasculature will be further clarified at the molecular level.

Materials and methods

Animals

C57BL/6 mice and ICR mice were purchased from Japan SLC (Shizuoka, Japan) at 8 weeks of age and used between 8 and 12 weeks of age. Ang1Tg mice (Suri *et al*, 1998) with a C57BL/6 background were provided by Dr GD Yanchopoulos (Regeneron Pharmaceuticals Inc., Tarrytown, NY). Animal care in our laboratory was in accordance with the guidelines of Kanazawa and Osaka University for animal and recombinant DNA experiments.

Plasmids and transfection

The mouse *Apelin* gene was cloned into the pCAGSIH expression vector. Lipofectamine Plus reagent (Invitrogen Life Technologies, Carlsbad, CA) was used to transfect cells with this plasmid and clones of cells exhibiting stable transfection were obtained by antibiotic resistance selection using G418 (Gibco, Grand Island, NY). Primer pairs for PCR to detect transfected gene are listed in Supplementary Table S1.

Tissue preparation, immunohistochemistry and flow cytometry

Tissue fixation, preparation of tissue sections and staining of sections or cultured cells with antibodies were performed as described previously (Takakura *et al*, 2000). An biotin-conjugated anti-CD31 mAb (Pharmingen, San Diego, CA), anti-apelin Ab (4G5; Kawamata *et al*, 2001) and anti-APJ polyclonal Ab were used in the staining of tissue sections or cultured cells. To obtain a specific antibody against mouse APJ, a rabbit was immunized with a synthetic peptide (CHEKSIPYSQETLVD) derived from the C-terminal region of APJ. Antisera were affinity purified with the same peptide. Preimmunized rabbit immunoglobulins were used as a negative control to confirm specific staining. Sections were counterstained with hematoxylin or propidium iodide. The sections were observed using an Olympus IX-70 microscope (Olympus, Tokyo, Japan) and images were acquired with a CoolSnap digital camera (Roper Scientific, Trenton, NJ). Whole-mount immunohistochemistry using anti-CD31 mAb or anti-APJ was performed as previously described (Takakura *et al*, 1998). Stained embryos were observed under a Leica MZ16FA stereomicroscope (Leica, Solms, Germany) and photographed with a DC120 digital camera (Pixera, Los Gatos, CA). In all assays, we used an isotype-matched control Ig as a negative control and confirmed that the positive signals were not derived from nonspecific background. Investigation of the density and morphology of microvessels in lectin-stained whole mount of tracheal blood vessels was performed as described (Yamada and Takakura, 2006). In brief, after anaesthesia with sodium pentobarbital, mice were injected into the tail vein with fluorescein-labelled *Lycopersicon esculentum* lectin (Vector Laboratories, Burlingame, CA), which binds uniformly to the luminal surface of ECs and adherent leukocytes. Lectin-stained tracheas were removed from apelin-deficient and WT mice and analysed under a fluorescence microscope. Images were processed using Adobe Photoshop 6.0 software (Adobe Systems, San Jose, CA). Flow cytometric analysis was performed as previously described (Yamada and Takakura, 2006). FITC-conjugated anti-CD45 mAb and PE-conjugated anti-CD31 mAb (Pharmingen) were used. The stained cells were analysed by FACS Calibur (Becton Dickinson, Franklin Lakes, NJ) and sorted by EPICS flow cytometer (ALTRA; Beckman Coulter, Fullerton, CA).

Cell culture

4×10^6 HUVECs were cultured in six-well plates for 12 h in Humedia EG2 (Kurabo, Osaka, Japan). Cells were then incubated in M199 medium supplemented with 1% fetal bovine serum (FBS). After 3 h of serum deprivation, cells were incubated with basal medium containing 500 ng/ml of Ang1 (R&D Systems, Minneapolis, MN), 100 ng/ml of apelin (Bachem, Bubendorf, Switzerland) or 20 ng/ml of VEGF-A_{165} (PeproTech, Rocky Hill, NJ).

The culture of P-Sp explant was performed as previously reported (Takakura *et al*, 2000). OP9 cells stably transfected with a pCAGSIH expression vector carrying the cDNA for mouse apelin or mock vector were used as feeder cells (OP9/apelin or OP9/vector, respectively) in the presence or absence of anti-apelin monoclonal blocking antibody (4G5; see Supplementary Figure 16 for functional analysis of this antibody in the inhibition of the apelin/APJ system) or control anti-B220 mAb. After 7 days of culture, the cultured cells on OP9 cells were fixed and stained with mAbs. For the culture of dissociated ECs from the AGM region, the regions were excised from E11.5 ICR embryos and dissociated by dispase II (Boehringer Mannheim, Mannheim, Germany) as previously described (Yamada and Takakura, 2006). Cells were suspended in DMEM supplemented with 15% fetal calf serum and cultured in OP9/vector or OP9/apelin seeded on 24-well plates in the presence of murine SCF (100 ng/ml; PeproTech), bFGF (1 ng/ml; R&D Systems) and OSM (10 ng/ml; R&D Systems). To this culture, we added 10 μg/ml anti-apelin or anti-B220 mAb. After 6 days of culture, the cells were fixed and double stained with anti-CD31 mAb and anti-VE-cadherin mAb (BD Pharmingen, San Jose, CA), or anti-CD31 mAb and claudin5 mAb (Abcam Inc., Cambridge, MA). Stained samples were analysed by confocal laser scanning microscopy (LSM510, Carl Zeiss, Germany). For the evaluation of apelin in promoting proliferation of HUVECs, HUVECs were cultured for 24 h in medium plus growth supplements and then for an additional 48 h in medium with or without apelin (10–100 ng/ml), VEGF (10 ng/ml) or apelin plus VEGF. Cell proliferation was then evaluated by directly counting the cell number.

Aortic ring culture for angiogenesis assay

Descending thoracic aortas were isolated from apelin-deficient mice. Under a stereomicroscope, multiple 1-mm-thick aortic rings were prepared. Rings were then placed between two layers of type I collagen gel (Cellmatrix Type IA, Nitta Zeratin, Osaka, Japan), supplemented with Medium 199, 20% FBS in the presence or absence of VEGF (20 ng/ml) or apelin (200 ng/ml). The cultures were kept at 37°C in a humidified environment for a week and examined every second day under an Olympus microscope (IX70).

Statistical analysis

All data are presented as mean ± standard deviation (s.d.). For statistical analysis, the statcel2 software package (OMS) was used with analysis of variance performed on all data followed by Tukey–Kramer multiple comparison test. When only two groups were compared, two-sided Student's *t*-test was used.

Supplementary data

Supplementary data are available at *The EMBO Journal* Online (http://www.embojournal.org).

Acknowledgements

We thank Dr GD Yanchopoulos (Regeneron Pharmaceuticals Inc.) and Dr Y Oike (Keio University, Tokyo, Japan) for providing us with Ang1Tg mice and with anti-LYVE-1 antibody, respectively. Moreover, we thank N Fujimoto for preparation of plasmid DNA and K Fukuhara for administrative assistance. This work was partly supported by a Grant-in-Aid from The Ministry of Education, Culture, Sports, Science and Technology of Japan to NT.

References

Adams RH, Wilkinson GA, Weiss C, Diella F, Gale NW, Deutsch U, Risau W, Klein R (1999) Roles of ephrinB ligands and EphB receptors in cardiovascular development: demarcation of arterial/venous domains, vascular morphogenesis, and sprouting angiogenesis. *Genes Dev* **13:** 295–306

Ashley EA, Powers J, Chen M, Kundu R, Finsterbach T, Caffarelli A, Deng A, Eichhorn J, Mahajan R, Agrawal R, Greve J, Robbins R, Patterson AJ, Bernstein D, Quertermous T (2005) The endogenous peptide apelin potently improves cardiac contractility and reduces cardiac loading *in vivo*. *Cardiovasc Res* **65:** 73–82

Carmeliet P (2003) Angiogenesis in health and disease. *Nat Med* **9:** 653–660

Cho CH, Kim KE, Byun J, Jang HS, Kim DK, Baluk P, Baffert F, Lee GM, Mochizuki N, Kim J, Jeon BH, McDonald DM, Koh GY

(2005) Long-term and sustained COMP-Ang1 induces long-lasting vascular enlargement and enhanced blood flow. *Circ Res* **97:** 86–94

Cox CM, D'Agostino SL, Miller MK, Heimark RL, Krieg PA (2006) Apelin, the ligand for the endothelial G-protein-coupled receptor, APJ, is a potent angiogenic factor required for normal vascular development of the frog embryo. *Dev Biol* **296:** 177–189

Croitoru-Lamoury J, Guillemin GJ, Boussin FD, Mognetti B, Gigout LI, Cheret A, Vaslin B, Le Grand R, Brew BJ, Dormont D (2003) Expression of chemokines and their receptors in human and simian astrocytes: evidence for a central role of TNF alpha and IFN gamma in CXCR4 and CCR5 modulation. *Glia* **41:** 354–370

Davis S, Aldrich TH, Jones PF, Acheson A, Compton DL, Jain V, Ryan TE, Bruno J, Radziejewski C, Maisonpierre PC, Yancopoulos GD (1996) Isolation of angiopoietin-1, a ligand for the TIE2 receptor, by secretion-trap expression cloning. *Cell* **87:** 1161–1169

De Mota N, Reaux-Le Goazigo A, El Messari S, Chartrel N, Roesch D, Dujardin C, Kordon C, Vaudry H, Moos F, Llorens-Cortes C (2004) Apelin, a potent diuretic neuropeptide counteracting vasopressin actions through inhibition of vasopressin neuron activity and vasopressin release. *Proc Natl Acad Sci USA* **101:** 10464–10469

Devic E, Paquereau L, Vernier P, Knibiehler B, Audigier Y (1996) Expression of a new G protein-coupled receptor X-msr is associated with an endothelial lineage in *Xenopus laevis*. *Mech Dev* **59:** 129–140

Devic E, Rizzoti K, Bodin S, Knibiehler B, Audigier Y (1999) Amino acid sequence and embryonic expression of msr/apj, the mouse homolog of *Xenopus* X-msr and human APJ. *Mech Dev* **84:** 199–203

Dumont DJ, Gradwohl G, Fong GH, Puri MC, Gerstenstein M, Auerbach A, Breitman ML (1994) Dominant-negative and targeted null mutations in the endothelial receptor tyrosine kinase, tek, reveal a critical role in vasculogenesis of the embryo. *Genes Dev* **8:** 1897–1909

Edinger AL, Hoffman TL, Sharron M, Lee B, Yi Y, Choe W, Kolson DL, Mitrovic B, Zhou Y, Faulds D, Collman RG, Hesselgesser J, Horuk R, Doms RW (1998) An orphan seven-transmembrane domain receptor expressed widely in the brain functions as a coreceptor for human immunodeficiency virus type 1 and simian immunodeficiency virus. *J Virol* **72:** 7934–7940

Ferrara N, Alitalo K (1999) Clinical applications of angiogenic growth factors and their inhibitors. *Nat Med* **5:** 1359–1364

Ferrara N, Gerber HP, LeCouter J (2003) The biology of VEGF and its receptors. *Nat Med* **9:** 669–676

Gale NW, Yancopoulos GD (1999) Growth factors acting via endothelial cell-specific receptor tyrosine kinases: VEGFs, angiopoietins, and ephrins in vascular development. *Genes Dev* **13:** 1055–1066

Gerhardt H, Betsholtz C (2003) Endothelial-pericyte interactions in angiogenesis. *Cell Tissue Res* **314:** 15–23

Inui M, Fukui A, Ito Y, Asashima M (2006) Xapelin and Xmsr are required for cardiovascular development in *Xenopus laevis*. *Dev Biol* **298:** 188–200

Ishida J, Hashimoto T, Hashimoto Y, Nishiwaki S, Iguchi T, Harada S, Sugaya T, Matsuzaki H, Yamamoto R, Shiota N, Okunishi H, Kihara M, Umemura S, Sugiyama F, Yagami K, Kasuya Y, Mochizuki N, Fukamizu A (2004) Regulatory roles for APJ, a seven-transmembrane receptor related to angiotensin-type 1 receptor in blood pressure *in vivo*. *J Biol Chem* **279:** 26274–26279

Jain RK (2005) Normalization of tumor vasculature: an emerging concept in antiangiogenic therapy. *Science* **307:** 58–62

Kasai A, Shintani N, Oda M, Kakuda M, Hashimoto H, Matsuda T, Hinuma S, Baba A (2004) Apelin is a novel angiogenic factor in retinal endothelial cells. *Biochem Biophys Res Commun* **325:** 395–400

Katugampola SD, Maguire JJ, Matthewson SR, Davenport AP (2001) [(125)I]-(Pyr(1))Apelin-13 is a novel radioligand for localizing the APJ orphan receptor in human and rat tissues with evidence for a vasoconstrictor role in man. *Br J Pharmacol* **132:** 1255–1260

Kawamata Y, Habata Y, Fukusumi S, Hosoya M, Fujii R, Hinuma S, Nishizawa N, Kitada C, Onda H, Nishimura O, Fujino M (2001) Molecular properties of apelin: tissue distribution and receptor binding. *Biochim Biophys Acta* **1538:** 162–171

Kleinz MJ, Davenport AP (2004) Immunocytochemical localization of the endogenous vasoactive peptide apelin to human vascular and endocardial endothelial cells. *Regul Pept* **118:** 119–125

Koller A, Huang A (1999) Development of nitric oxide and prostaglandin mediation of shear stress-induced arteriolar dilation with aging and hypertension. *Hypertenston* **34:** 1073–1079

Korff T, Augustin HG (1998) Integration of endothelial cells in multicellular spheroids prevents apoptosis and induces differentiation. *J Cell Biol* **143:** 1341–1352

Lawson ND, Vogel AM, Weinstein BM (2002) sonic hedgehog and vascular endothelial growth factor act upstream of the Notch pathway during arterial endothelial differentiation. *Dev Cell* **3:** 127–136

Lindahl P, Johansson BR, Leveen P, Betsholtz C (1997) Pericyte loss and microaneurysm formation in PDGF-B-deficient mice. *Science* **277:** 242–245

Liu Y, Cox SR, Morita T, Kourembanas S (1995) Hypoxia regulates vascular endothelial growth factor gene expression in endothelial cells. Identification of a 5' enhancer. *Circ Res* **77:** 638–643

Masri B, Knibiehler B, Audigier Y (2005) Apelin signalling: a promising pathway from cloning to pharmacology. *Cell Signal* **17:** 415–426

O'Dowd BF, Heiber M, Chan A, Heng HH, Tsui LC, Kennedy JL, Shi X, Petronis A, George SR, Nguyen T (1993) A human gene that shows identity with the gene encoding the angiotensin receptor is located on chromosome 11. *Gene* **136:** 355–360

Oettgen P (2001) Transcriptional regulation of vascular development. *Circ Res* **89:** 380–388

Okamoto R, Ueno M, Yamada Y, Takahashi N, Sano H, Suda T, Takakura N (2005) Hematopoietic cells regulate the angiogenic switch during tumorigenesis. *Blood* **105:** 2757–2763

Risau W (1997) Mechanisms of angiogenesis. *Nature* **386:** 671–674

Saint-Geniez M, Masri B, Malecaze F, Knibiehler B, Audigier Y (2002) Expression of the murine msr/apj receptor and its ligand apelin is upregulated during formation of the retinal vessels. *Mech Dev* **110:** 183–186

Sato TN, Tozawa Y, Deutsch U, Wolburg-Buchholz K, Fujiwara Y, Gendron-Maguire M, Gridley T, Wolburg H, Risau W, Qin Y (1995) Distinct roles of the receptor tyrosine kinases Tie-1 and Tie-2 in blood vessel formation. *Nature* **376:** 70–74

Scott IC, Masri B, D'Amico LA, Jin SW, Jungblut B, Wehman AM, Baier H, Audigier Y, Stainier DY (2007) The G protein-coupled receptor agtrl1b regulates early development of myocardial progenitors. *Dev Cell* **12:** 403–413

Simon MC (2004) Vascular morphogenesis and the formation of vascular networks. *Dev Cell* **6:** 479–482

Suri C, Jones PF, Patan S, Bartunkova S, Maisonpierre PC, Davis S, Sato TN, Yancopoulos GD (1996) Requisite role of angiopoietin-1, a ligand for the Tie-2 receptor, during embryonic angiogenesis. *Cell* **87:** 1171–1180

Suri C, McClain J, Thurston G, McDonald DM, Zhou H, Oldmixon EH, Sato TN, Yancopoulos GD (1998) Increased vascularization in mice overexpressing angiopoietin-1. *Science* **282:** 468–471

Szokodi I, Tavi P, Foldes G, Voutilainen-Myllyla S, Ilves M, Tokola H, Pikkarainen S, Piuhola J, Rysa J, Toth M, Ruskoaho H (2002) Apelin, the novel endogenous ligand of the orphan receptor APJ, regulates cardiac contractility. *Circ Res* **91:** 434–440

Takakura N, Huang XL, Naruse T, Hamaguchi I, Dumont DJ, Yancopoulos GD, Suda T (1998) Critical role of the TIE2 endothelial cell receptor in the development of definitive hematopoiesis. *Immunity* **9:** 677–686

Takakura N, Watanabe T, Suenobu S, Yamada Y, Noda T, Ito Y, Satake M, Suda T (2000) A role for hematopoietic stem cells in promoting angiogenesis. *Cell* **102:** 199–209

Tatemoto K, Hosoya M, Habata Y, Fujii R, Kakegawa T, Zou MX, Kawamata Y, Fukusumi S, Hinuma S, Kitada C, Kurokawa T, Onda H, Fujino M (1998) Isolation and characterization of a novel endogenous peptide ligand for the human APJ receptor. *Biochem Biophys Res Commun* **251:** 471–476

Tatemoto K, Takayama K, Zou MX, Kumaki I, Zhang W, Kumano K, Fujimiya M (2001) The novel peptide apelin lowers blood pressure via a nitric oxide-dependent mechanism. *Regul Pept* **99:** 87–92

Thurston G, Wang Q, Baffert F, Rudge J, Papadopoulos N, Jean-Guillaume D, Wiegand S, Yancopoulos GD, McDonald DM (2005) Angiopoietin 1 causes vessel enlargement, without angiogenic

sprouting, during a critical developmental period. *Development* **132:** 3317–3326

Wang HU, Chen ZF, Anderson DJ (1998) Molecular distinction and angiogenic interaction between embryonic arteries and veins revealed by ephrin-B2 and its receptor Eph-B4. *Cell* **93:** 741–753

Yamada Y, Takakura N (2006) Physiological pathway of differentiation of hematopoietic stem cell population into mural cells. *J Exp Med* **203:** 1055–1065

Zhong TP, Childs S, Leu JP, Fishman MC (2001) Gridlock signalling pathway fashions the first embryonic artery. *Nature* **414:** 216–220

EMBO
reports

scientific report

Conformational switch of angiotensin II type 1 receptor underlying mechanical stress-induced activation

Noritaka Yasuda[1], Shin-ichiro Miura[2]*, Hiroshi Akazawa[1,3]*, Toshimasa Tanaka[4], Yingjie Qin[1], Yoshihiro Kiya[2], Satoshi Imaizumi[2], Masahiro Fujino[2], Kaoru Ito[1], Yunzeng Zou[5], Shigetomo Fukuhara[6], Satoshi Kunimoto[6], Koichi Fukuzaki[7], Toshiaki Sato[7], Junbo Ge[5], Naoki Mochizuki[6], Haruaki Nakaya[7], Keijiro Saku[2] & Issei Komuro[1+]*

[1]Department of Cardiovascular Science and Medicine, Chiba University Graduate School of Medicine, Chuo-ku, Chiba, Japan, [2]Department of Cardiology, Fukuoka University School of Medicine, Jonan-ku, Fukuoka, Japan, [3]Division of Cardiovascular Pathophysiology, Chiba University Graduate School of Medicine, Chuo-ku, Chiba, Japan, [4]Pharmaceutical Research Division, Discovery Research Center, Takeda Pharmaceutical Company Limited, Yodogawa-ku, Osaka, Japan, [5]Shanghai Institute of Cardiovascular Diseases, Zhongshan Hospital, Fudan University, Shanghai, China, [6]Department of Structural Analysis, National Cardiovascular Center Research Institute, Suita, Osaka, Japan, and [7]Department of Pharmacology, Chiba University Graduate School of Medicine, Chuo-ku, Chiba, Japan

The angiotensin II type 1 (AT_1) receptor is a G protein-coupled receptor that has a crucial role in the development of load-induced cardiac hypertrophy. Here, we show that cell stretch leads to activation of the AT_1 receptor, which undergoes an anticlockwise rotation and a shift of transmembrane (TM) 7 into the ligand-binding pocket. As an inverse agonist, candesartan suppressed the stretch-induced helical movement of TM7 through the bindings of the carboxyl group of candesartan to the specific residues of the receptor. A molecular model proposes that the tight binding of candesartan to the AT_1 receptor stabilizes the receptor in the inactive conformation, preventing its shift to the active conformation. Our results show that the AT_1 receptor undergoes a conformational switch that couples mechanical stress-induced activation and inverse agonist-induced inactivation.

[1]Department of Cardiovascular Science and Medicine, Chiba University Graduate School of Medicine, 1-8-1 Inohana, Chuo-ku, Chiba 260-8670, Japan
[2]Department of Cardiology, Fukuoka University School of Medicine, 7-45-1, Nanakuma, Jonan-ku, Fukuoka 814-0180, Japan
[3]Division of Cardiovascular Pathophysiology, Chiba University Graduate School of Medicine, 1-8-1 Inohana, Chuo-ku, Chiba 260-8670, Japan
[4]Pharmaceutical Research Division, Discovery Research Center, Takeda Pharmaceutical Company Limited, 2-17-85 Juso-Honmachi, Yodogawa-ku, Osaka, 532-8686, Japan
[5]Shanghai Institute of Cardiovascular Diseases, Zhongshan Hospital, Fudan University, 180 Feng Lin Road, Shanghai 200032, China
[6]Department of Structural Analysis, National Cardiovascular Center Research Institute, 5-7-1 Fujishirodai, Suita, Osaka 565-8565, Japan
[7]Department of Pharmacology, Chiba University Graduate School of Medicine, 1-8-1 Inohana, Chuo-ku, Chiba 260-8670, Japan
*These authors contributed equally to this work
+Corresponding author. Tel: +81 43 226 2097; Fax: +81 43 226 2557;
E-mail: komuro-tky@umin.ac.jp

Received 20 June 2007; revised 27 November 2007; accepted 28 November 2007; published online 18 January 2008

Keywords: cardiac hypertrophy; G protein-coupled receptor; inverse agonist; mechanical stress; molecular model
EMBO reports (2008) 9, 179–186. doi:10.1038/sj.embor.7401157

INTRODUCTION

Mechanical stress to cardiomyocytes is the most important stimulus that triggers hypertrophic responses (Komuro & Yazaki, 1993), and the hypertrophic responses to mechanical stretch are significantly inhibited by pretreatment with angiotensin II (AngII) type 1 (AT_1) receptor blockers (ARB; Sadoshima *et al*, 1993; Yamazaki *et al*, 1995). Therefore, the AT_1 receptor is crucial in the development of load-induced cardiac hypertrophy. We have recently shown that mechanical stress leads to activation of the AT_1 receptor without the involvement of AngII (Zou *et al*, 2004). Mechanical stretch did not activate extracellular signal-regulated protein kinases (ERKs) in human embryonic kidney (HEK) 293 cells with no detectable expression of AT_1 receptor, but forced expression of the AT_1 receptor conferred the ability to respond to stretch. Candesartan, an ARB, inhibited mechanical stress-induced AT_1 receptor activation and pressure overload-induced hypertrophy even in angiotensinogen-null mice. However, it remains unclear how AT_1 receptor detects mechanical stress and translates it into biochemical signals inside the cells, and how candesartan inhibits AngII-independent activation of AT_1 receptor.

Here, we show that there is a change in the conformation of the AT_1 receptor when activated by mechanical stress. We refer to this as a 'stretch-induced' conformational change, but whether the AT_1 receptor directly absorbs the mechanical energy that drives this conformational change remains unclear. Studies using substituted cysteine accessibility mapping (SCAM) showed that transmembrane (TM) 7 of the AT_1 receptor showed an anticlockwise

Fig 1 | Mechanical stress-induced anticlockwise rotation of TM7 in the AT_1 receptor. (A) Alteration of cysteine accessibility by mechanical stretch in HEK293-AT_1 cells. Cell membranes were prepared before (0 min) and after the indicated stretch time, and subjected to a SCAM study. $^*P<0.05$ versus 0 min. (B) Alteration of cysteine accessibility by mechanical stretch in COS7 cells expressing wild-type (WT) and mutant AT_1 receptors. The cells were stretched for 8 min. Cys(−) represents a mutant receptor in which all the cysteine residues were replaced with alanine. $^*P<0.05$ versus stretch (−), $^\#P<0.05$ versus stretch (−) in wild-type, $^\S P<0.05$ versus stretch (−) in Cys76Ala/Cys289Ala. (C) Alteration of cysteine accessibility by mechanical stretch in COS7 cells expressing Cys76Ala/Cys289Ala mutant receptors in which TM7 residues ranging from Thr 287 to Asn 295 were successively substituted to cysteine. $^*P<0.05$ versus stretch (−), $^\#P<0.05$ versus stretch (−) in Cys76Ala/Cys289Ala. (D) Helical wheel representation of TM7 reporter cysteine residues and the pattern of their reactivity to $MTSEA^+$. Positions of $MTSEA^+$-reacted cysteine residues in TM7 that affected ^{125}I-labelled (Sar^1, Ile^8) AngII binding are shown in a helical wheel representation viewed from the extracellular side without (left) or with (right) stretch. Black circles correspond to the residues that inhibited ^{125}I-labelled (Sar^1, Ile^8) AngII binding by 50% or more when substituted to cysteine, whereas dark grey circles indicate those that inhibited by around 30%. Light grey circles indicate those that had no inhibitory effect. White circles indicate receptors that were not examined. AngII, angiotensin II; AT_1, AngII type 1; $MTSEA^+$, methanethiosulphonate ethyl-ammonium; SCAM, substituted cysteine accessibility mapping; TM7, transmembrane 7.

rotation and a shift into the ligand-binding pocket in response to mechanical stretch. Candesartan suppressed the stretch-induced helical movement of TM7, and the binding of the carboxyl group of candesartan to Gln257 in TM6 and Thr287 in TM7 was responsible for the potent inverse agonism. Our results provide a previously unknown basis for the structural switch of the AT_1 receptor that couples mechanical stress-induced activation and inverse agonist-induced inactivation.

RESULTS AND DISCUSSION

First, by using immunofluorescence analysis, we confirmed that the AT_1 receptor was localized predominantly in the plasma membrane of HEK293 cells expressing this receptor (HEK293-AT_1 cells) before and after stretch (supplementary Fig S1 online). Next, to examine whether mechanical stretch can induce changes in the conformation of the AT_1 receptor, we carried out a SCAM study with or without stretch. The SCAM study has been used to investigate relative conformational changes by validating the presence of cysteine residues within the ligand pocket (see supplementary information online). As we reported previously (Miura *et al*, 2003), the percentage inhibition of ^{125}I-labelled (Sar^1, Ile^8) AngII binding by methanethiosulphonate ethyl-ammonium ($MTSEA^+$) reagent was approximately 30% in HEK293-AT_1 cells, because Cys76 in TM2 is accessible to water within the ligand pocket (Fig 1A). We found that the percentage inhibition of ^{125}I-labelled (Sar^1, Ile^8) AngII gradually increased after stretch, reaching approximately 60% after 8 min (Fig 1A), indicating that stretch induces a conformational change in the AT_1 receptor. To identify the native cysteine residues that gain accessibility to $MTSEA^+$, we replaced individual cysteine residues with alanine and analysed the accessibility with or without stretch (Fig 1B). The affinities of these mutants for ^{125}I-labelled (Sar^1, Ile^8) AngII were equivalent to that of the wild-type receptor (supplementary Table S1 online). Consistent with our previous results (Miura & Karnik, 2002; Miura *et al*, 2003), the reactions to $MTSEA^+$ were enhanced in the Cys296Ala mutant, because this mutation increases the accessibility of Cys289 without altering the accessibility of Cys76 (Fig 1B). Interestingly, Cys289Ala, Cys76Ala/Cys289Ala, Cys76Ala/Cys289Ala/Cys296Ala and Cys(−) mutants, which contain a cysteine to alanine mutation at Cys289 in TM7, did not show a stretch-induced increase in percentage inhibition of ^{125}I-labelled (Sar^1, Ile^8) AngII binding. These results indicate that mechanical stretch increases the accessibility of Cys289 by inducing a change in the conformation of TM7.

To determine the stretch-induced helical movement of TM7, we carried out a series of SCAM experiments by using Cys76Ala/Cys289Ala mutant receptors in which TM7 residues ranging from Thr287 to Asn295 were substituted with cysteine one at a time. Cys76Ala/Ile288Cys/Cys289Ala and Cys76Ala/Cys289Ala/Ala291Cys mutants showed higher percentage inhibitions than Cys76Ala/Cys289Ala (Fig 1C), indicating that Ile288 and Ala291 are accessible to the ligand-binding pocket. Stretch increased accessibility in Cys76Ala (Cys289) and in Cys76Ala/Ile288Cys/Cys289Ala mutants, but decreased it in the Cys76Ala/Cys289Ala/Ala291Cys mutant (Fig 1C). These results indicate that mechanical stress induces anticlockwise rotation of TM7 (Fig 1D). In general, G protein-coupled receptors (GPCRs) are maintained in an inactive conformation by interhelical interactions that constrain the receptor structure (Gether, 2000). Although interactions between TM3 and TM6 might be a conserved mechanism for conformational stabilization of GPCRs (Gether, 2000; Yao *et al*, 2006), stabilizing interactions between TM3 and TM7 have been reported in the AT_1 receptor (Groblewski *et al*, 1997). Relaxation of the constraining interhelical interactions triggers activation of GPCRs when bound to agonists; therefore, we propose that the stabilizing interaction between TM3 and TM7 in the AT_1 receptor might be disrupted by mechanical stress independently of AngII and that the anticlockwise rotation of TM7 might cause activation of intracellular signalling pathways.

As shown in Fig 2A, candesartan completely suppressed a stretch-induced increase in the percentage inhibition of ^{125}I-labelled (Sar^1, Ile^8) AngII binding in the SCAM experiments, indicating that candesartan blocked mechanical stress-induced conformational change in the AT_1 receptor. ARBs show diverse inhibitory patterns ranging from surmountable inhibition (parallel rightward shift of agonist concentration–response curves) to insurmountable inhibition (waning of the maximal response; Vauquelin *et al*, 2001). We found that a derivative of candesartan (candesartan-7H), which lacks the carboxyl group at the benzimidazole ring (Fig 2B), showed a much lower inhibitory effect than candesartan on AngII-induced activation of ERKs in HEK293-AT_1 cells, with a rightward shift of the concentration–response curve (Fig 2C). Importantly, 1×10^{-5} M of candesartan-7H inhibited almost equally the activation of ERKs induced by 1×10^{-7} M of AngII as did 1×10^{-7} M of candesartan (Fig 2D). However, stretch-induced ERK activations were inhibited by 1×10^{-7} M of candesartan, but not by candesartan-7H even at 1×10^{-5} M (Fig 2D). Consistently, candesartan-7H did not show a

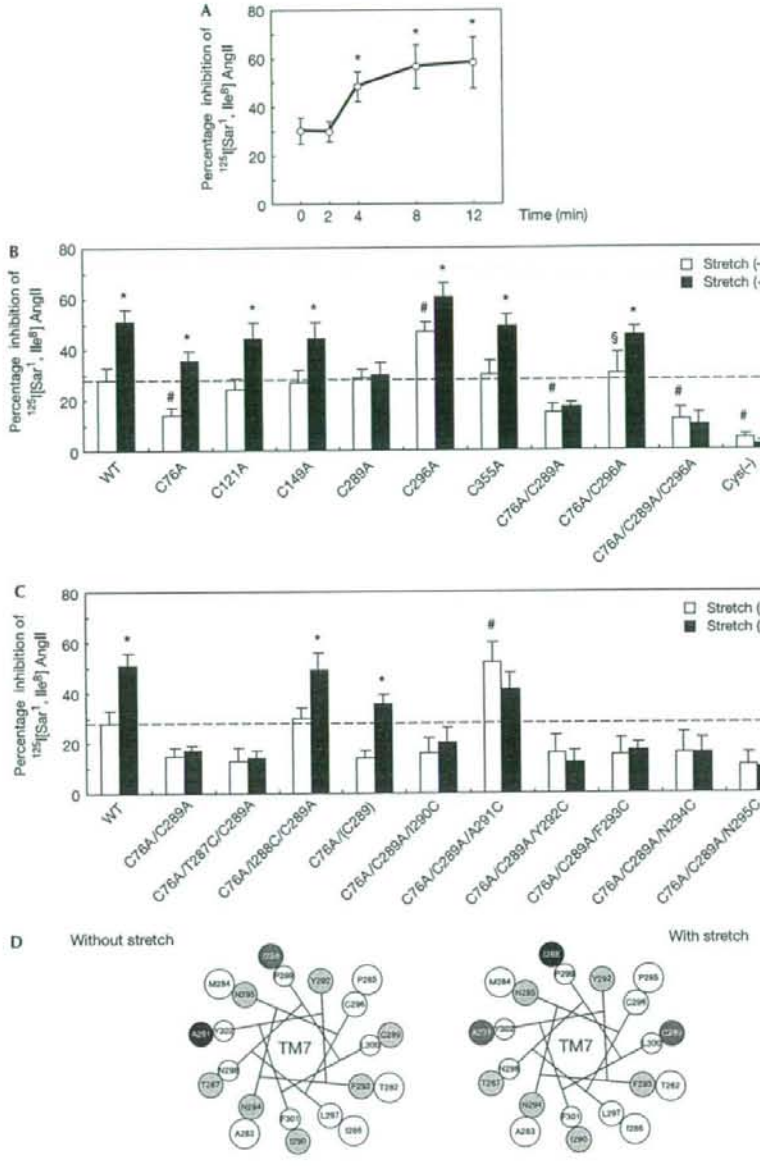

suppressive effect on stretch-induced increase in the percentage inhibition of ^{125}I-labelled (Sar^1, Ile^8) AngII binding in the SCAM experiments (Fig 2A). In addition, candesartan, but not candesartan-7H, reduced the basal activity of wild-type AT_1 receptor or a constitutively active AT_1-N111G mutant, which contains an Asn 111 to glycine mutation (Boucard *et al*, 2003; supplementary Fig S2 online). These results indicate that the carboxyl group of candesartan is responsible both for the insurmountable inhibition of AngII-dependent receptor activation and for the potent inverse agonism against AngII-independent receptor activation.

To establish the specific amino acids that bind to the the carboxyl group of candesartan, we selected candidate residues—His 256, Gln 257, Thr 287 and Tyr 292—on the basis of a molecular model of the AT_1 receptor (Noda *et al*, 1995; Takezako *et al*, 2004)

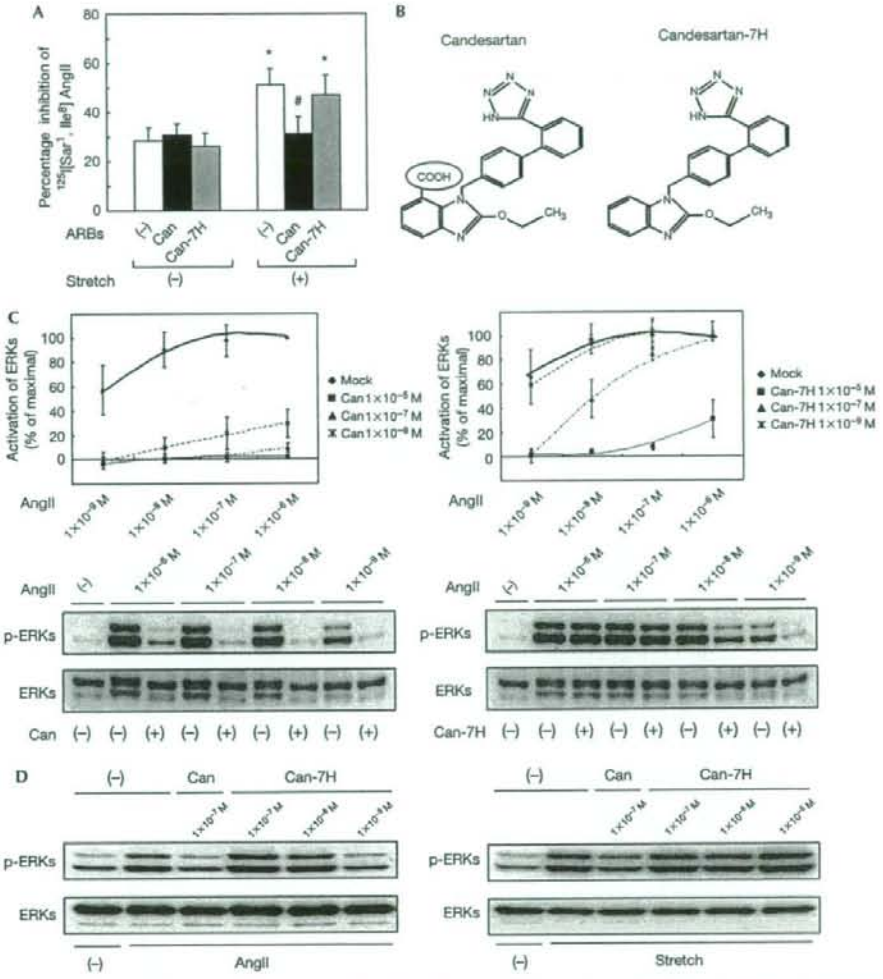

Fig 2 | The carboxyl group is a crucial structure for inverse agonism of candesartan. (A) Alteration of cysteine accessibility by mechanical stretch with or without ARBs in HEK293-AT_1 cells. The cells were pretreated with 1×10^{-7} M candesartan (Can) or its derivative, candesartan-7H (Can-7H), and then stretched for 0 or 8 min. $^*P<0.05$ versus stretch (−), $^\#P<0.05$ versus stretch (+) without pretreatment of Can. **(B)** Chemical structures of Can and Can-7H. Can contains a carboxyl group at the benzimidazole ring (circled COOH), whereas Can-7H does not have this structure. **(C)** Response curves of AngII-mediated activation of ERKs (upper panels). HEK293-AT_1 cells were pretreated with 1×10^{-7} M of Can or Can-7H and stimulated by AngII at the indicated concentrations (lower panels). The activation of ERKs was determined by using a polyclonal antibody against phosphorylated ERKs (p-ERKs). **(D)** HEK293-AT_1 cells were pretreated with the indicated concentrations of Can or Can-7H and stimulated by AngII (left) or mechanical stretch (right). The activation of ERKs was determined. AngII, angiotensin II; ARB, AT_1 receptor blocker; AT_1, AngII type 1; ERK, extracellular signal-regulated protein kinase; HEK, human embryonic kidney cells.

and examined the binding affinities of candesartan to AT_1 mutant receptors with a substitution of each candidate residue to alanine. The affinities of candesartan were reduced by approximately tenfold in Gln257Ala and Thr287Ala mutants compared with the wild-type receptor (supplementary Table S2 online), indicating that the interactions of the carboxyl group of candesartan with Gln 257 and Thr 287 might be involved in a tight drug–receptor binding. Insurmountable inhibition by candesartan was not observed in these AT_1 receptor mutants, because candesartan could not suppress the activation of ERKs mediated by higher concentration

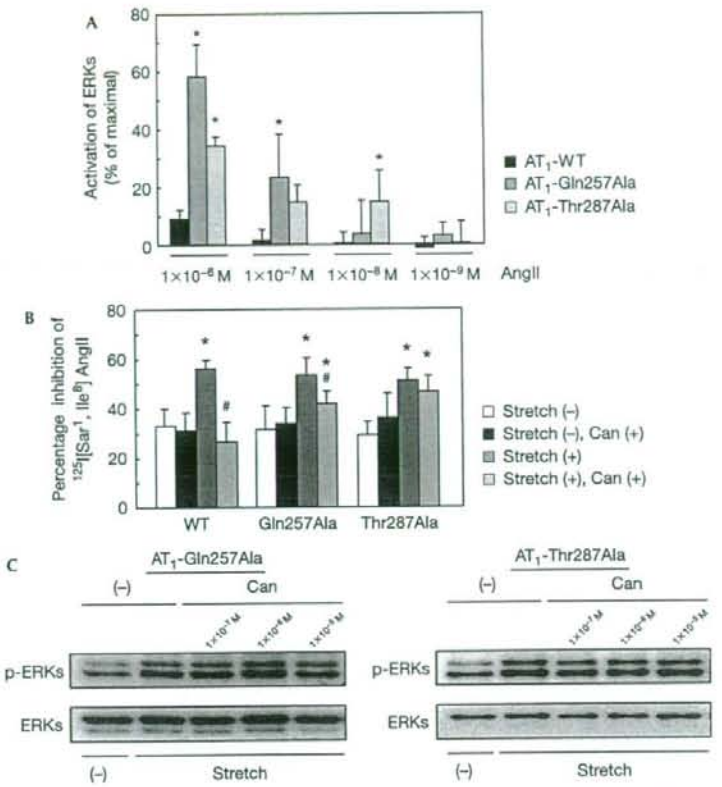

Fig 3 | Interactions of the carboxyl group of candesartan with Gln 257 and Thr 287 in the AT_1 receptor. (A) HEK293 cells expressing wild-type AT_1, Gln257Ala or Thr287Ala mutant receptors were pretreated with 1×10^{-7} M of candesartan (Can) and stimulated by AngII at the indicated concentrations. The activation of ERKs was determined. $^*P<0.05$ versus wild-type AT_1. **(B)** Alteration of cysteine accessibility by mechanical stretch in COS7 cells expressing wild-type AT_1, Gln257Ala or Thr287Ala receptors. The cells were pretreated with or without 1×10^{-7} M Can and stretched for 0 or 8 min. $^*P<0.05$ versus stretch (–), $^\#P<0.05$ versus stretch (+) in each receptor. **(C)** HEK293 cells expressing Gln257Ala (left) or Thr287Ala (right) mutant receptor were pretreated with the indicated concentrations of Can and stimulated by mechanical stretch. The activation of ERKs was determined. AngII, angiotensin II; AT_1, AngII type 1; ERK, extracellular signal-regulated protein kinase; HEK, human embryonic kidney cells.

of AngII in HEK293 cells expressing these mutants (Fig 3A). Furthermore, we found that Gln257Ala and Thr287Ala mutants, similar to the wild-type receptor, showed an increase in the percentage inhibition of ^{125}I-labelled (Sar^1, Ile^8) AngII binding after stretch, which was not significantly suppressed by candesartan (Fig 3B). In addition, inverse agonist activity of candesartan was also abolished in Gln257Ala and Thr287Ala mutants, because candesartan could not inhibit the stretch-induced activation of ERKs in HEK293 cells expressing these mutants (Fig 3C). Collectively, these results indicate that the tight binding of the carboxyl group of candesartan to Gln 257 and Thr 287 in AT_1 receptor is crucial for the potent inverse agonism.

Finally, we constructed molecular models on three states: (i) AT_1 receptor model without stretch, (ii) AT_1 receptor model with stretch, and (iii) AT_1 receptor with stretch in the presence of candesartan (Fig 4A; see supplementary information online). As shown in Fig 1C, mechanical stress induced anticlockwise rotation of TM7 and eventually the Cys 289 residue, originally faced in the direction of TM1, became accessible to the ligand-binding pocket. As Ile 288 becomes more accessible after stretch, TM7 might shift inside the ligand-binding pocket. By contrast, TM7 would shift away from the ligand-binding pocket in a constitutively active AT_1-N111G mutant (Boucard *et al*, 2003). We reported previously that an amino–aromatic bonding interaction between Asn 111 in TM3 of the AT_1 receptor and Tyr 4 of AngII triggers AngII-dependent receptor activation (Miura *et al*, 1999), and that the AT_1-N111G receptor mimics the state of the wild-type receptor partly activated by AngII (Miura & Karnik, 2002). Therefore, an active conformation of the AT_1 receptor induced by mechanical stress might be substantially different from that in AngII-dependent receptor activation. The 'AT_1 receptor model with stretch in the presence of candesartan' fulfils both

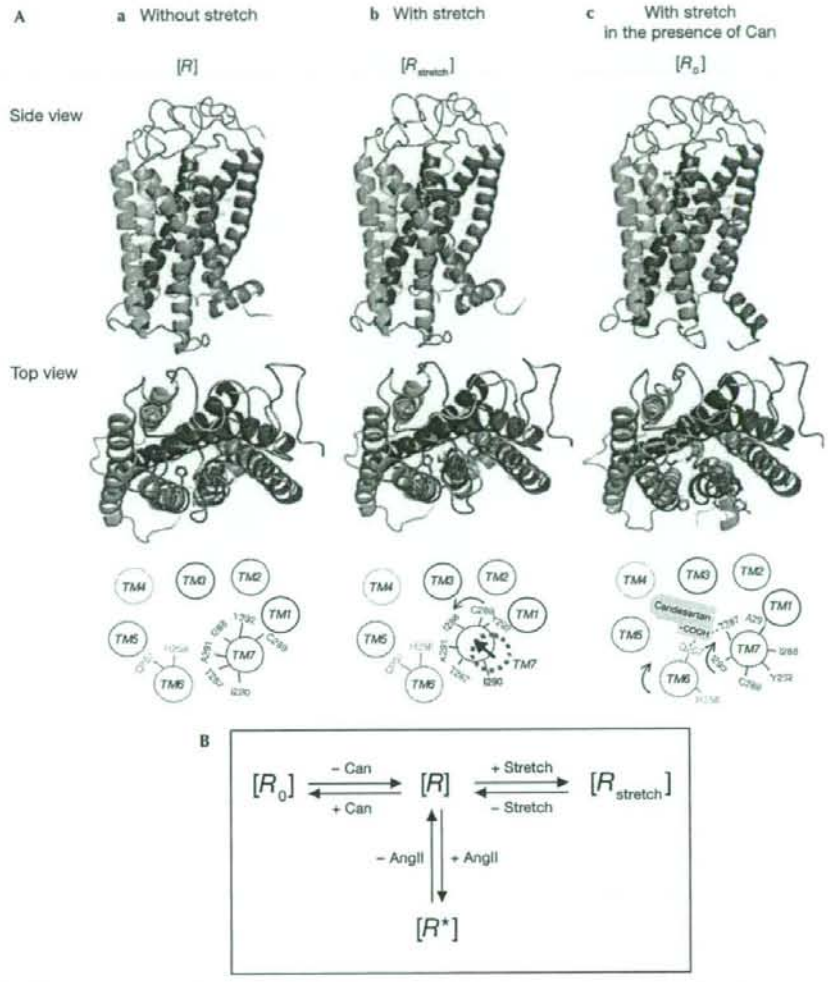

Fig 4 | Molecular model of stretch-induced changes in the conformation of the AT_1 receptor. (**A**) A molecular model was constructed with three states: AT_1 receptor model without stretching, with stretch and with stretch in the presence of candesartan (Can). (**B**) The AT_1 receptor is predicted to adopt distinct conformations. [*R*] is an unaligned inactive state and [R_0] is an inactive state stabilized by an inverse agonist candesartan. [*R**] is an active state stabilized by the agonist AngII and [$R_{stretch}$] is another active state stabilized by mechanical stretch. AngII, angiotensin II; AT_1, AngII type 1.

conditions in which the tetrazole group of candesartan binds to Lys 199 (Noda *et al*, 1995; Takezako *et al*, 2004) and in which the carboxyl group of candesartan stably forms two hydrogen bonds with the side chains of Gln 257 and Thr 287.

According to a sequential binding and conformational model for the molecular mechanism of ligand action on GPCRs (Gether, 2000), the unaligned receptor exists in a unique state [*R*] that can undergo transitions to at least two other stabilized states, [R_0] and [*R**]. [R_0] is an inactive state of the AT_1 receptor that is stabilized by an inverse agonist candesartan, and [*R**] is an active state stabilized by AngII (Fig 4A,B). Mechanical stretch might stabilize the AT_1 receptor to another active state [$R_{stretch}$], independently of AngII (Fig 4A,B). In this study, the carboxyl group of candesartan was found to bind to Gln 257 in TM6 and to Thr 287 in TM7, and these interactions might constrain two TM domains until the receptor is stabilized in the inactive state [R_0]. According to the model of mechanical stress in the presence of candesartan, TM6 rotates clockwise and TM7 moves to the same position in the inactive state [*R*] with clockwise rotation (Fig 4A). The clockwise rotations of TM6 and TM7 in this model were consistent with

the result of a SCAM experiment showing a decrease in the accessibility of His 256, an increase in the accessibility of Ile 290 and a decrease in the accessibility of Ala 291 to the ligand-binding pocket (supplementary Fig S3 online). The distances the carboxyl group of candesartan from the hydroxyl group of Thr 287 and the carboxyl group of Gln 257 are 2.06 Å and 2.09 Å, respectively, which are reasonable for causing interactions through electrostatic and/or hydrogen bonds.

Here, we have shown compelling evidence that the AT_1 receptor shows a conformational switch when mechanical stress of the whole cell leads to receptor activation. Recent evidence has shown that mechanical force directly alters the conformation or folding of cytoskeletal proteins, which enhances enzymatic activities or susceptibility to enzymatic reactions (Sawada *et al*, 2006). However, mechanical stretch activated the AT_1 receptor even when the actin cytoskeleton was disorganized by treatment with cytochalasin D (supplementary Fig S4 online). Alternatively, stretch-activated ion channels (SACs) might trigger activation of the AT_1 receptor after stretch. Although the rapid changes of membrane potential or intracellular Ca^{2+} within seconds of the initiation of stretching could not be measured, we found that treatment with GsMtx-4, a specific blocker for SACs, did not inhibit stretch-induced activation of the AT_1 receptor (supplementary Fig S5 online). It will be of particular interest to describe the precise mechanism through which mechanical force is directly or indirectly transmitted to the AT_1 receptor. Reconstitution of a mechanosensitive channel of large conductance from *Escherichia coli* (Perozo *et al*, 2002) in synthetic phosphatidylcholines with different chain lengths showed that a thin bilayer favoured the open state of channels, whereas a thick bilayer stabilized the closed state. In addition, a recent study using a fluorescence resonance energy transfer approach showed that membrane fluidity affected the conformational dynamics of the bradykinin B2 receptor in endothelial cells (Chachisvilis *et al*, 2006). It might be possible that membrane tension causes thinning of the lipid bilayer, which triggers tilting of TM7 in the AT_1 receptor to avoid hydrophobic mismatch and to rectify a lateral pressure profile (Orr *et al*, 2006).

Furthermore, our present study provides a structural basis for how inverse agonists can inhibit receptor activation in the absence of agonists. According to our molecular model (Fig 4A,B), candesartan, as an inverse agonist, might forcibly induce a distinct transition from $[R]$ to an inactive conformation $[R_0]$, preventing the shift of equilibrium to an active conformation $[R_{stretch}]$, which translates mechanical stress into the activation of ERKs through phosphorylation of Janus kinase 2 and Gq protein coupling (Zou *et al*, 2004). This is consistent with the result of a recent study that used a fluorescence resonance energy transfer approach and showed that agonists and inverse agonists for α2A-adrenergic receptor induced distinct conformational changes in the receptor (Vilardaga *et al*, 2005). Recently, we reported that potent inverse agonism of olmesartan to suppress the constitutive activity of the AT_1-N111G receptor required cooperative interactions between olmesartan and Tyr 113 in TM3 and His 256 in TM6 (Miura *et al*, 2006). Many drugs, previously considered to be neutral antagonists, have been shown to behave as an inverse agonist for GPCRs. Therefore, elucidation of the molecular basis of inverse agonism is of great importance to pharmacotherapy targeted GPCRs.

METHODS

Application of mechanical stretch. The passive stretch of cultured cells by 20% was conducted as described previously (Zou *et al*, 2004; supplementary Fig S6 online).

Substituted cysteine accessibility mapping. SCAM was carried out as described previously (Miura & Karnik, 2002; Miura *et al*, 2003, 2005).

Molecular modelling of the AT_1 receptor. Amino-acid sequence alignment between the human AT_1 receptor and bovine rhodopsin was carried out using the CLUSTAL W program. Homology model structures of the human AT_1 receptor were then constructed based on the crystal structure of bovine rhodopsin (Protein Data Bank ID: 1F88) by using the homology module in the Insight II program package (Accelrys Inc, San Diego, CA, USA). Conformations of extracellular loops were constructed by using the Search/Generate-Loops function of Insight II (see supplementary information online). The complete structure was subjected to energy minimization using the MMFF94 × force field in the programme MOE (version 2005.06, Chemical Computing Group) with a harmonic force constraint against the initial atomic positions to prevent the large movement of TM helices. Further methods can be found in the supplementary information online.

Supplementary information is available at *EMBO reports* online (http://www.emboreports.org).

ACKNOWLEDGEMENTS

We are grateful to Dr S.S. Karnik for providing cDNAs. This work was supported, in part, by grants from the Japanese Ministry of Education, Science, Sports and Culture (to I.K., S.-i.M. and H.A.); from Health and Labor Sciences Research Grants, Japan Health Sciences Foundation, Takeda Medical Research Foundation, Takeda Science Foundation, Uehara Memorial Foundation, Kato Memorial Trust for Nambyo Research and the Japan Medical Association (to I.K.); and from Mochida Memorial Foundation, Japanese Heart Foundation/Novartis Research Award on Molecular and Cellular Cardiology, and Japan Intractable Diseases Research Foundation (to H.A.).

REFERENCES

Boucard AA, Roy M, Beaulieu ME, Lavigne P, Escher E, Guillemette G, Leduc R (2003) Constitutive activation of the angiotensin II type 1 receptor alters the spatial proximity of transmembrane 7 to the ligand-binding pocket. *J Biol Chem* **278:** 36628–36636

Chachisvilis M, Zhang YL, Frangos JA (2006) G protein-coupled receptors sense fluid shear stress in endothelial cells. *Proc Natl Acad Sci USA* **103:** 15463–15468

Gether U (2000) Uncovering molecular mechanisms involved in activation of G protein-coupled receptors. *Endocr Rev* **21:** 90–113

Groblewski T, Maigret B, Larguier R, Lombard C, Bonnafous JC, Marie J (1997) Mutation of Asn111 in the third transmembrane domain of the AT_1A angiotensin II receptor induces its constitutive activation. *J Biol Chem* **272:** 1822–1826

Komuro I, Yazaki Y (1993) Control of cardiac gene expression by mechanical stress. *Annu Rev Physiol* **55:** 55–75

Miura S, Karnik SS (2002) Constitutive activation of angiotensin II type 1 receptor alters the orientation of transmembrane Helix-2. *J Biol Chem* **277:** 24299–24305

Miura S, Feng YH, Husain A, Karnik SS (1999) Role of aromaticity of agonist switches of angiotensin II in the activation of the AT_1 receptor. *J Biol Chem* **274:** 7103–7110

Miura S, Zhang J, Boros J, Karnik SS (2003) TM2–TM7 interaction in coupling movement of transmembrane helices to activation of the angiotensin II type-1 receptor. *J Biol Chem* **278:** 3720–3725

Miura S, Karnik SS, Saku K (2005) Constitutively active homo-oligomeric angiotensin II type 2 receptor induces cell signaling independent of receptor conformation and ligand stimulation. *J Biol Chem* **280:** 18237–18244

Miura S *et al* (2006) Molecular mechanism underlying inverse agonist of angiotensin II type 1 receptor. *J Biol Chem* **281:** 19288–19295

Noda K, Saad Y, Kinoshita A, Boyle TP, Graham RM, Husain A, Karnik SS (1995) Tetrazole and carboxylate groups of angiotensin receptor antagonists bind to the same subsite by different mechanisms. *J Biol Chem* **270:** 2284–2289

Orr AW, Helmke BP, Blackman BR, Schwartz MA (2006) Mechanisms of mechanotransduction. *Dev Cell* **10:** 11–20

Perozo E, Cortes DM, Sompornpisut P, Kloda A, Martinac B (2002) Open channel structure of MscL and the gating mechanism of mechanosensitive channels. *Nature* **418:** 942–948

Sadoshima J, Xu Y, Slayter HS, Izumo S (1993) Autocrine release of angiotensin II mediates stretch-induced hypertrophy of cardiac myocytes *in vitro*. *Cell* **75:** 977–984

Sawada Y, Tamada M, Dubin-Thaler BJ, Cherniavskaya O, Sakai R, Tanaka S, Sheetz MP (2006) Force sensing by mechanical extension of the Src family kinase substrate p130Cas. *Cell* **127:** 1015–1026

Takezako T, Gogonea C, Saad Y, Noda K, Karnik SS (2004) 'Network leaning' as a mechanism of insurmountable antagonism of the angiotensin II type 1 receptor by non-peptide antagonists. *J Biol Chem* **279:** 15248–15257

Vauquelin G, Fierens F, Verheijen I, Vanderheyden P (2001) Insurmountable AT(1) receptor antagonism: the need for different antagonist binding states of the receptor. *Trends Pharmacol Sci* **22:** 343–344

Vilardaga JP, Steinmeyer R, Harms GS, Lohse MJ (2005) Molecular basis of inverse agonism in a G protein-coupled receptor. *Nat Chem Biol* **1:** 25–28

Yamazaki T *et al* (1995) Angiotensin II partly mediates mechanical stress-induced cardiac hypertrophy. *Circ Res* **77:** 258–265

Yao X, Parnot C, Deupi X, Ratnala VR, Swaminath G, Farrens D, Kobilka B (2006) Coupling ligand structure to specific conformational switches in the β2-adrenoceptor. *Nat Chem Biol* **2:** 417–422

Zou Y *et al* (2004) Mechanical stress activates angiotensin II type 1 receptor without the involvement of angiotensin II. *Nat Cell Biol* **6:** 499–506

11. Na^+/H^+ 交換輸送体：機能調節と薬物標的としての意義

中村(西谷)友重・古林創史・久光　隆・岩田裕子・若林繁夫

Na^+/H^+ 交換輸送体（Na^+/H^+ exchanger：NHE，SLC9[用語1]）は，細胞内pH，Na^+濃度，細胞容積の調節など，イオン環境整備に関わる主要なトランスポーターである。NHEによるイオン輸送は，ストレス時に分泌されるホルモンやメカニカル刺激など様々なシグナルにより活性化されるため，薬物標的として特に重要である。そのため古くからNHE特異的阻害薬が開発され，各種心疾患や癌を含む多くの疾病におけるNHEの関与が報告されてきた。本稿では，特にNHE1の活性化が心肥大・心不全発症に十分な要因になりうるという著者らの最近の知見を中心に述べ，形質膜で起こるトランスポーターの活性変化が遺伝子発現までをも制御し，組織リモデリングを惹起する最初のシグナルになりうることを紹介する。

はじめに

トランスポーターは細胞にとって最初の玄関口であり，種々のイオンや栄養物質を厳密に選別したうえで細胞内に運び入れたり，また有害物質を細胞外に排出するといった重要な役割を果たしている。このトランスポーターがもつ厳格な選択性と細胞膜局在による細胞外からの容易なアクセスは，創薬を考えるうえで大変重要な性質である。Na^+/H^+交換輸送体（NHE）は細胞内pH（pH_i），Na^+濃度，細胞容積の調節などのイオン環境整備に関わる主要なトランスポーターである。以前からアミロライド誘導体などNHEの特異的阻害薬が開発され，心疾患を含む様々な病態との関連が研究されてきた。NHEはホルモン・増殖因子・機械的刺激などあらゆる細胞外シグナルによって活性化を受ける。その卓越した制御機構は，病態を生む背景として重要である。また最近，NHEは細胞膜の限局した領域（ラフト）に局在し，細胞外マイクロ環境におけるH^+制御に重要であるとする状況証拠が出されており，疾患との関連においても新たな潮流になる可能性がある。本稿では，NHEアイソフォーム（NHE1～11）のうち普遍型NHE1に限定して分子と活性制御に関する最近のトピックスを簡単に紹介したのち，NHE1と心疾患との関連について著者らの知見を中心に述べたい。

Ⅰ．NHE1分子と活性制御

NHE1分子は膜貫通領域を含むN末側の輸送を担うドメインとC末側の制御を担う大きな細胞質ドメインの2つに大きく分けることができる（図❶）[1,2]。後者にはカルシニューリンB様タンパク質（CHP）[3]，カルモデュリンなどのタンパ

key words
トランスポーター，Na^+/H^+交換輸送体（NHE），Na^+/Ca^{2+}交換輸送体（NCX1），
カリポライド，細胞内Ca^{2+}過負荷，トランスジェニック，心肥大，心不全，
カルシニューリン(CN)/NFAT経路，CaMKⅡ/HDAC経路，Ca^{2+}依存性心肥大シグナル

図❶　NHE1分子および相互作用するタンパク質

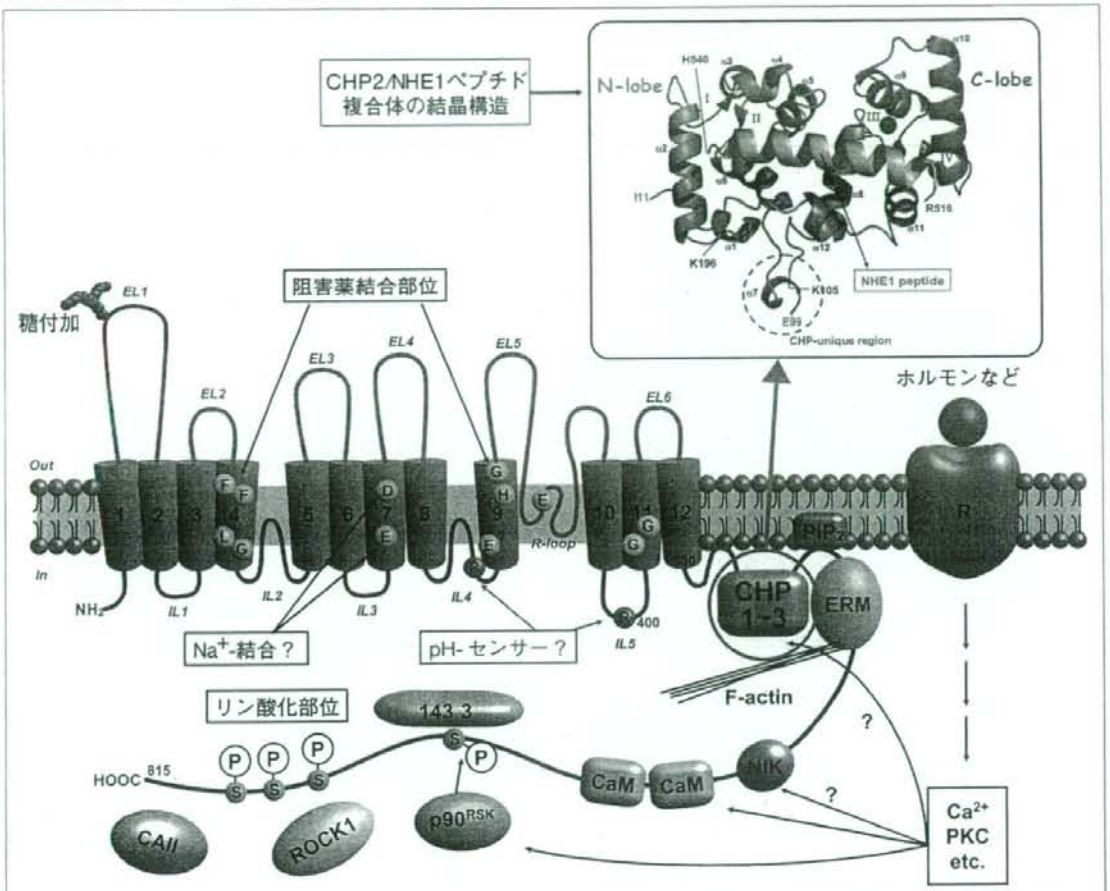

挿入図は，NHEの必須制御因子であるCHP2とNHE1の細胞質領域との複合体の原子構造モデルである。NIK：Nck結合キナーゼ，ROCK1：Rhoキナーゼ1，PIP_2：ホスファチジルイノシトール二リン酸，CAⅡ：カーボニックアンヒドラーゼⅡ，PKC：プロテインキナーゼC，CaM：カルモデュリン，R：受容体，R-loop：再陥入ループ，EL：細胞外ループ，IL：細胞内ループ

（グラビア頁参照）

ク質やイノシトールリン脂質（PIP_2）など様々な制御因子が結合する。CHPはNHE1（NHE 2～5もまた）の構造・機能の維持に必須なCa^{2+}結合モチーフを有するサブユニットタンパク質である。NHE1はダイマーを形成するので[4]，形質膜上ではNHE1/CHPヘテロダイマーがさらに二量体を形成すると考えられる。最近，著者らはCHPとNHE1側の結合ドメインとの複合体の結晶構造を2.7Åの解像度で明らかにし，両者の相互作用の詳細を明らかにした[5]。NHE1は生理的にはNa^+ポンプによって形成されるNa^+濃度勾配に従って1：1ストイキオメトリーでH^+を排出する系であるが，分子の細胞質側には「pHセンサー[用解2]」と呼ばれるH^+制御部位が存在し，ホルモン刺激などに応じてそのH^+感受性が変化する。

NHE1の疾患との関連で重要なことは，NHE1が細胞外液性因子やメカニカルストレスなどあらゆる刺激によって活性化されるという事実である。NHE1が活性化されてまず起こることは，①細胞内アルカリ化，②細胞内Na^+濃度上昇，③細胞外酸性化という3つのイオン変化である（図❷）。細胞内アルカリ化は種々の酵素活性の上昇をもたらし，細胞増殖，分化，遊走，分泌，筋収縮などの細胞機能を亢進する。癌細胞ではNHE1

図❷ NHE1の活性化に伴うイオン変化と生理機能

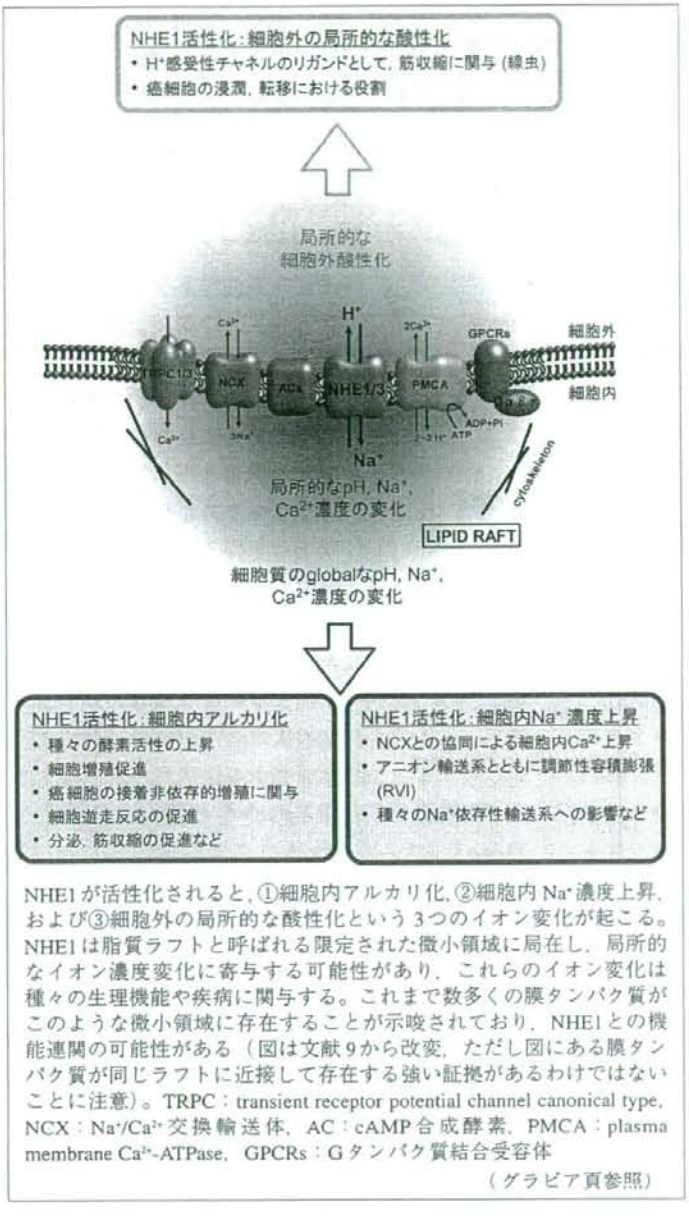

NHE1が活性化されると，①細胞内アルカリ化，②細胞内 Na^+ 濃度上昇，および③細胞外の局所的な酸性化という3つのイオン変化が起こる。NHE1は脂質ラフトと呼ばれる限定された微小領域に局在し，局所的なイオン濃度変化に寄与する可能性があり，これらのイオン変化は種々の生理機能や疾病に関与する。これまで数多くの膜タンパク質がこのような微小領域に存在することが示唆されており，NHE1との機能連関の可能性がある（図は文献9から改変，ただし図にある膜タンパク質が同じラフトに近接して存在する強い証拠があるわけではないことに注意）。TRPC：transient receptor potential channel canonical type，NCX：Na^+/Ca^{2+} 交換輸送体，AC：cAMP合成酵素，PMCA：plasma membrane Ca^{2+}-ATPase，GPCRs：Gタンパク質結合受容体

（グラビア頁参照）

が恒常的に活性化されており，正常細胞に比べて静止時の pH_i が7.2～7.7と異常に高い。他方，細胞内 Na^+ 濃度上昇は容積調節に関与するほか，心筋などの興奮性細胞では Na^+/Ca^{2+} 交換輸送体（NCX1）の逆モードを促進し細胞内 Ca^{2+} 過負荷をもたらす（後述）。最近，著者らはこの機構による Ca^{2+} 過負荷がまた筋ジストロフィー[用語]の筋変性にも関わることを報告した[6]。これまでのNHE1に関する研究は細胞内イオン濃度変化にのみ着目していたが，近年NHEによって細胞外に排出される H^+ が注目されるようになった。最近，線虫の腸管細胞に存在するNHE1（PBO-4）によって微小間隙に排出された H^+ が筋肉細胞の H^+ 感受性チャネル（PBO-5/6）活性化のシグナルとして利用されるという興味深い報告がなされた[7]。また，癌細胞では細胞内外のpH勾配が逆転しており，細胞外間隙の著しい酸性化（pH_i = 6.2～6.8）によって細胞外マトリクスは消化され，癌細胞の浸潤・転移が促される[8]。

NHE1のこれら生理・病態との関連で注目すべきことは，いくつかの状況証拠からNHE1がラフトと呼ばれる細胞膜の限局した領域に局在する可能性が高いという点である。ラフトは脂質組成が他の形質膜とは異なる限局した領域であり，しばしばカベオリンのような足場タンパク質によって細胞内に陥入する。こうしたマイクロドメインにおけるNHE1の局在は細胞内外の微小領域内の H^+，Na^+ 濃度あるいは二次的に Ca^{2+} 濃度を大きく変動させ，近傍に存在する種々の酵素や膜タンパク質の機能に影響を与える可能性がある。実際にcAMP合成酵素（AC）はpH感受性であるために，NHE1近傍に存在することによって高い活性を維持できるという[9]。こうした概念はNHE1の生理機能と病態的役割を理解するために重要であるが，確定するためにはまだ多くの説得力のある研究が必要だろう。

図❸　活性化型 NHE1 高発現による心筋リモデリングとそのメカニズム

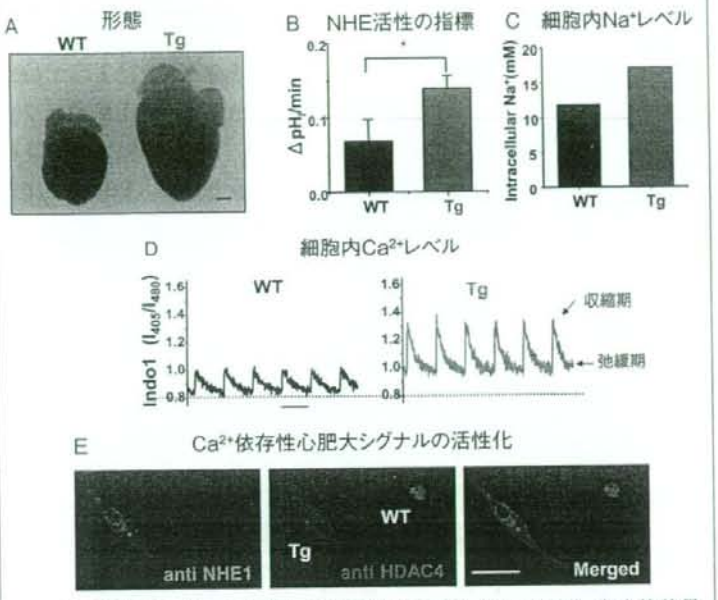

A. 自己阻害ドメインを欠損した活性化型 NHE1（Δ637-656）を心筋特異的に高発現する Tg マウスは心肥大および拡張型心筋症の様相を呈する（いずれも生後 100 日齢）。スケールバー：1 mm。

B. NHE1 活性の 1 つの指標である細胞内酸性化の後の pH_i 回復の速度は Tg 由来の心筋細胞で有意に上昇。

C. 細胞内 Na^+ 濃度は 11.9mM（WT）から 17.1mM（Tg）と 1.5 倍に上昇（Null point 法により測定）。

D. 収縮期，弛緩期の細胞内 Ca^{2+} 濃度および Ca^{2+} トランジェントの振幅は，いずれも Tg 由来の心筋細胞で増加。

E. Tg 心筋における Ca^{2+} 依存性心肥大シグナル CaMKⅡ/HDAC 経路の活性化。WT および Tg 由来の新生児培養マウス心筋細胞の混合培養系において，NHE 1 高発現細胞（Tg）では HDAC は核外に，WT では核内に局在していた。スケールバー：20 μm。　（グラビア頁参照）

Ⅱ．NHE1 と心疾患

NHE1 は心筋においても主要な H^+ 排出機構であり，心筋収縮を阻害する細胞内アシドーシスなどの際，速やかに活性化され pH_i を維持したり，そのほか細胞内 Na^+ 濃度や細胞容積の調節などの恒常性維持をつかさどっている。ところが近年，虚血-再灌流障害を受けた心筋において NHE1 の発現や活性の亢進が認められ，さらに NHE1 の特異的阻害薬が障害を軽減することから，NHE1 がこの疾患の重要なメディエータであるとする説が数多くある[10]。実際，NHE1 欠損マウスでは心筋虚血-再灌流障害[用解4]に対し抵抗性があることが報告されている[11]。また NHE1 の活性化が，急性の虚血-再灌流障害のみならず遺伝子発現変化を伴う心肥大や心筋リモデリング[用解5]などにも寄与している可能性が指摘されている。例えば，抗利尿ホルモン（ANP）受容体欠損マウスや β1 アドレナリン受容体高発現トランスジェニック（Tg）マウスで認められる心肥大，心筋線維化および心不全が，NHE1 の特異的阻害薬カリポライドにより軽減されることなどである[12][13]。しかし，このようなマウス心筋では受容体刺激などを伴う複数のシグナル経路が同時に活性化されており，NHE1 の活性化そのものが心肥大・心不全を引き起こす最初のシグナルになりうるのか，また NHE1 の活性化に伴いどのようなシグナル伝達経路が活性化されるのかなど明らかでなかった。

これらを明らかにするため，著者らは自己阻害ドメインを欠損した活性化型 NHE1（Δ637-656）[14]を心筋特異的に高発現する Tg マウスを作製した[15]。Tg マウス心筋は生後 20～40 日齢で心肥大を呈し（図❸ A），さらに拡張型心筋症の様相を示した。また心エコーによる解析から，Tg 心筋では心機能低下ならびに不整脈が認められ死亡率も顕著に増加していた。このような NHE1 活性化による心筋リモデリングの分子メカニズムを明らかにするため単離心筋細胞を用いて検討を行ったところ，Tg 由来単離心筋細胞では pH_i および Na^+ 濃度の上昇とともに，収縮・弛緩期両方における細胞内 Ca^{2+} 濃度（$[Ca^{2+}]_i$）が顕著に増加していた（図❸ B-D）。弛緩期の $[Ca^{2+}]_i$ 上昇は Na^+/Ca^{2+} 交換系との機能連関を介した Na^+ 依存性 Ca^{2+} 過負荷によるものと考えられる。$[Ca^{2+}]_i$ は主

図❹ NHE1 活性化による心筋リモデリングの推定される細胞内シグナリング

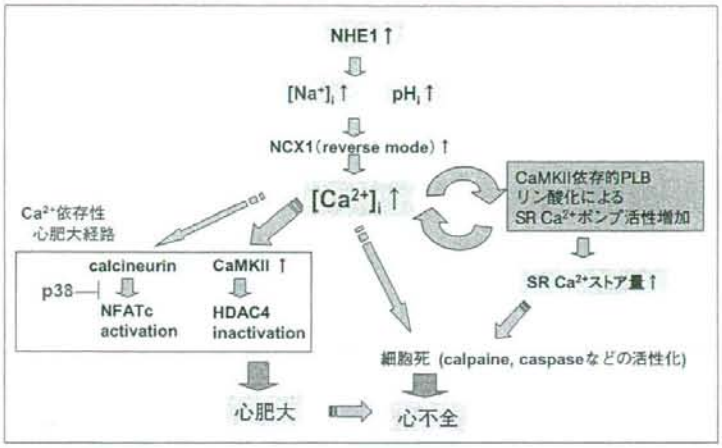

に筋小胞体 SR からの Ca^{2+} 取り込みと流出により制御されていることから関連因子の活性化状態を Tg と WT とで比較したところ，Tg 心筋では $[Ca^{2+}]_i$ の上昇に伴いカルモデュリンキナーゼⅡ（CaMKⅡ）が活性化され，それは SR Ca^{2+} ポンプ（SERCA）の制御因子であるホスホランバン（PLB）のリン酸化および Ca^{2+} 遊離チャネルの活性化を促し，結果的に Ca^{2+} ポンプ活性上昇による Ca^{2+} ストア量の増大，引き続く SR からの Ca^{2+} 流出の上昇により収縮期の Ca^{2+} が増加することがわかった。Tg 心筋におけるこのような SR Ca^{2+} ハンドリングの変化は，細胞外からの持続的な Ca^{2+} 流入とともに SR の Ca^{2+} 過負荷を引き起こし，最終的に細胞死を導くと考えられる。実際にヒトの不全心で認められるのと同様，Tg 由来の単離心筋細胞における収縮力は高速刺激時には $[Ca^{2+}]_i$ が高いにもかかわらず減少しており，筋原線維の Ca^{2+} 感受性低下による心機能不全が細胞レベルで生じていることが確認された。

さらに Tg マウスでは，Ca^{2+} 依存性心肥大シグナル用解6因子 CaMKⅡおよびカルシニューリン（CN）の著明な活性化が認められた。これらタンパク質の活性化はそれぞれ下流の転写制御因子 HDAC および NFAT 経路の活性化を介して（CN/NFAT 経路および CaMKⅡ/HDAC 経路）心肥大遺伝子発現を惹起することが知られている。興味深いことに，ラット培養心筋細胞で NHE1 を高発現すると，カリポライド依存的な HDAC のほぼ完全な核外移行および NFAT の核内移行が認められた。Tg マウス心筋細胞においても同様に HDAC の核外移行が観察されたが（図❸E），一方 NFAT の活性化は部分的であり，これは心肥大抑制因子 p38 の活性化によるものと考えられた。これら NHE1 高発現による *in vivo*，*in vitro* の変化はカリポライドにより有意に抑制された。

以上の結果をまとめると，NHE1 活性化により心肥大・心不全が生じることがわかった。そのメカニズムとして，細胞内 Na^+ 濃度，引き続く細胞内 Ca^{2+} 濃度の増加が生じ，これは，CaMKⅡおよび CN を活性化するが，Tg 心筋では p38 が特に活性化されているため，主に CaMKⅡ-HDAC 経路を介して心肥大が導かれると考えられる。他方，細胞内 Ca^{2+} 濃度の増加は，CaMKⅡによる PLB のリン酸化，SERCA の活性化を介して SR の Ca^{2+} 量を増加させ，このポジティブフィードバックが細胞死を引き起こし，心不全へと導くと考えられる（図❹）。このことは NHE1 の活性化が，遺伝子発現を変化させ心肥大・心不全を発症させる Ca^{2+} シグナルを惹起するのに十分であるという新しい概念を提示する[15]。

おわりに

上述したように，NHE はその生理機能が広範囲の疾患に関与するため，薬効標的として古くから注目され，およそ 20 年以上にわたって特異的な阻害薬が改善を重ねて開発されてきた。確かにカリポライドなどの NHE 阻害薬は心疾患動物の著明な病態改善をもたらすが，心臓病患者を対象としたヒト臨床評価では必ずしも意図した効果は得られていない。危惧されるのは，NHE を完全に抑制することによって Na^+ 蓄積を阻害する一方で，酸排出という生理的に重要な機能をも抑制してしまうことになりかねないことである。したが